FEBS Letters 582 (2008) 1335–1340

Role of side-chains in the operation of the main molecular hinge of 3-phosphoglycerate kinase

Judit Szabó[a,1], Andrea Varga[a,1], Beáta Flachner[a], Peter V. Konarev[b,c], Dmitri I. Svergun[b,c], Péter Závodszky[a], Mária Vas[a,*]

[a] *Institute of Enzymology, Biological Research Center, Hungarian Academy of Sciences, H-1518 Budapest, P.O. Box 7, Hungary*
[b] *EMBL Outstation, c/o DESY, Notkestrasse 85, 22603 Hamburg, Germany*
[c] *Institute of Crystallography, Russian Academy of Sciences, Leninsky pr. 59, 117333 Moscow, Russia*

Received 30 January 2008; revised 14 February 2008; accepted 12 March 2008

Available online 20 March 2008

Edited by Miguel De la Rosa

Abstract The single mutants (F165A, E192A, F196A, S392A, T393A) at and near the main hinge (β-strand L) of human 3-phosphoglycerate kinase (hPGK) exhibit variously reduced enzyme activity, indicating the cumulative effects of these residues in regulating domain movements. The residues F165 and E192 are also essential in maintaining the conformational integrity of the whole molecule, including the hinge-region. Shortening of βL by deleting T393 has led to a dramatic activity loss and the concomitant absence of domain closure (as detected by small angle X-ray scattering), demonstrating the role of βL in functioning of hPGK. The role of each residue in the conformational transmission is described.

Keywords: Domain movement; Hinge; 3-Phosphoglycerate kinase; Site-directed mutagenesis; Small angle X-ray scattering

1. Introduction

3-Phosphoglycerate-kinase (PGK) is a typical hinge-bending enzyme. The present study is underlined by the currently renewed interest in the structural changes involved in protein function [1,2]. PGK catalyzes the phospho-transfer from 1,3-BPG to MgADP producing 3-PG and MgATP during glycolysis. One of the two substrates, 3-PG [3] or 1,3-BPG binds to the N-domain, while the nucleotide substrate, MgATP [4] or MgADP [5] binds to the C-domain. There are several lines of evidences that domain closure is required for catalysis. In the well-structured interdomain region the β-strand L was assigned as the main hinge of PGK [6] (Fig. 1A). Involvement of βL in a substrate induced double sided H-bond network appeared to be a plausible mechanism of operation of this hinge [7]. The atomic contacts (H-bonds) of the conserved Ser and Thr side-chains of βL, indeed, vary during transition from open to closed conformation (Fig. 1B). Thus, one can assume an essential role of these side-chains in operation of βL. In order to test this hypothesis, we have replaced these and the surrounding side-chains into Ala. In previous mutagenesis studies with yeast PGK the role of the salt bridge between E192 and H390 (hPGK numbering, Fig. 2) has been probed in this region and found not to be responsible for domain closure [8]. Among the present mutants we have also produced E192A and in its surroundings F165A and F196A in order to test the importance of their hydrophobic contacts in the interdomain region. The residue F196 is not fully conserved, but it has a hydrophobic nature in all sequences (e.g. Leu in *Thermotoga maritima* PGK, shown in Fig. 2D). Proton NMR investigation of F196L and F196W mutants [9] revealed the importance of F196 for the mobility of the interdomain region. We also produced a double mutant (S392A–T393A) to test the cumulative effects of the mutations, as well as a deletion mutant (T393del) to probe the requirement of the complete βL sequence for domain closure. The mutants of hPGK were characterised in functional (enzyme kinetic, substrate binding) and in structural (CD, DSC, SAXS) investigations. The results supported the assumption that βL operates as the main molecular hinge of PGK. The role of each investigated residue in mediating the domain movement is described.

2. Materials and methods

2.1. Chemicals

Na-salts of 3-PG, ATP and ADP were from Boehringer. The substrates MgATP and MgADP were formed by mixing $MgCl_2$ (Sigma) and ATP or ADP, respectively, as described earlier [4]. NADH, NADP and glucose were from Sigma. 1,3-BPG was prepared as described by Furfine and Velick [11]. Isopropyl β-D-thiogalactopyranoside (Fermentas), chloramphenicol and ampicillin (Sigma) were used for the fermentation. Primers were produced by Invitrogen. The Ellman's reagent (Nbs_2) was from Serva.

2.2. Enzymes

The hPGK was produced, purified and stored as described previously [10]. Concentration of hPGK solution was determined using ε_{280} value of 27960 M^{-1} cm^{-1}. Auxiliary enzymes were from Sigma.

2.3. Site-directed mutagenesis

Residues 165, 192, 196, 392, 393 and 398 of hPGK were mutated into Ala using QuikChange site-directed mutagenesis kit (Stratagene). The mutations were checked by DNA sequencing.

*Corresponding author. Fax: +36 1 466 5465.
E-mail address: vas@enzim.hu (M. Vas).

[1]These authors contributed equally to the work.

Abbreviations: AMP-PNP, β,γ-imido-adenosine-5′ triphosphate; 3-PG, 3-phosphoglycerate; 1,3-BPG, 1,3-bisphosphoglycerate; CD, circular dichroism; DSC, differential scanning calorimetry; Nbs_2, Ellman's reagent, 5,5′-dithiobis-(2-nitrobenzoic acid); PGK, 3-phospho-D-glycerate kinase (EC 2.7.2.3); hPGK, human PGK; SAXS, small angle X-ray scattering

0014-5793/$34.00
doi:10.1016/j.febslet.2008.03.016

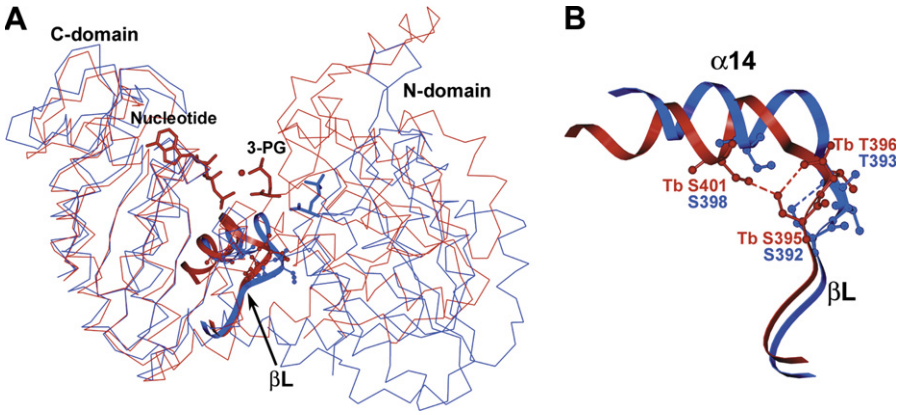

Fig. 1. βL operates as the main hinge of PGK. The Cα traces of the molecules of open conformation of the 3-PG binary complex of pig muscle (blue, [3]) and the closed conformation of MgADP*3-PG ternary complex of *Trypanosoma brucei* (red, [17]) PGKs are superimposed according to the core β-sheets of the C-terminal domain. The βL and α14 in both structures are highlighted by ribbons, the substrates and certain side-chains are shown by stick and ball and stick models, respectively. In panel (B) the details around βL are enlarged.

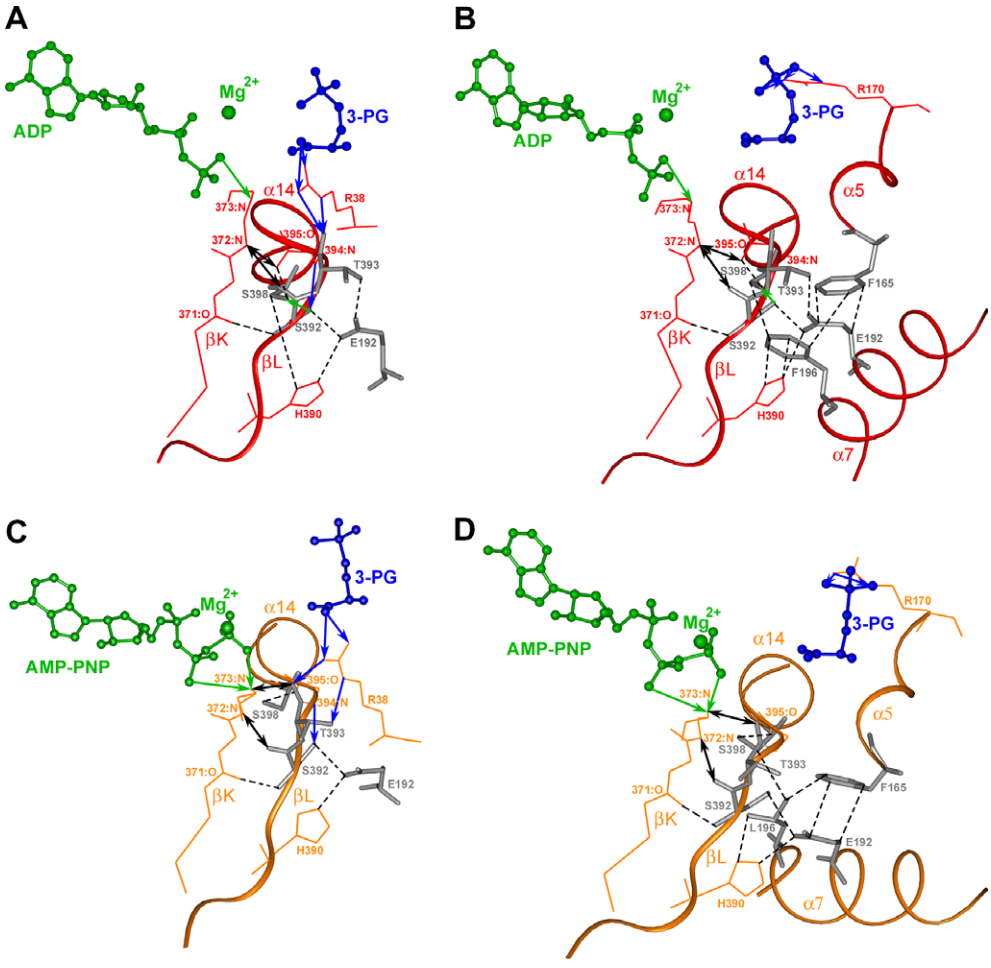

Fig. 2. Details of the main hinge-region of PGK. The atomic interactions in the closed conformations of the ternary complexes of MgADP∗3-PG of *Trypanosoma brucei* ([17], panels A and B) and of MgAMP-PNP∗3-PG of *Thermotoga maritima* ([18], panels C and D) are illustrated. 3-PG and the nucleotide are shown by blue and green ball and stick models, respectively. The atomic contacts formed upon 3-PG and nucleotide binding are illustrated by arrows with the respective colours. Other structural parts of the proteins are coloured as red and orange for *Trypanosoma brucei* (panels A and B) and *Thermotoga maritima* (panels C and D) PGK structures, respectively. Side-chains are numbered according to the hPGK sequence. The mutated side-chains are highlighted by grey stick models. The permanent interactions are shown by dashed black lines. The H-bonds formed only in the ternary complexes are indicated by black double-sided arrows.

2.4. CD spectroscopy

The measurements were carried out with Jasco 720 spectropolarimeter in both far (200–260 nm) and near (260–350 nm) UV regions. The spectra were measured at 20 °C, using 0.1 and 1 cm path length cells, at 0.009 and 0.056 mM (0.4 and 2.5 mg/ml) protein concentrations, respectively.

2.5. Differential scanning calorimetry (DSC) experiments

The measurements were carried out in a MicroCal VP-DSC type microcalorimeter (MicroCal Inc.) with a cell volume of 0.51 ml, at constant scan rate of 1 K/min. In all experiments carefully degassed solutions of 0.003 mM (0.13 mg/ml) protein were used. The data were analyzed using MicroCal Origin 5.0 software.

2.6. Enzyme kinetic studies

The activity of hPGK was measured as described earlier [10]. For the reaction with the substrates 3-PG and MgATP the rate equation describing activation by the excess of the substrate [12] was used for analysis of the data. Activity measurements with the substrates 1,3-BPG and MgADP were analysed using the Michaelis–Menten equation. All kinetic experiments were carried out at 20 °C in 20 mM Tris/HCl buffer, pH 7.5, containing 1 mM dithiotreitol.

2.7. Thiol-reactivity studies

The time courses of thiol modification of PGK were followed using Nbs_2 as described earlier [13].

2.8. SAXS measurements and data processing

Synchrotron radiation X-ray scattering data were collected on the X33 beamline at the Hamburg EMBL Outstation [14] as described earlier [7]. Solutions of hPGK of 0.1–0.3 mM (5–15 mg/mL) in the storage buffer, and the ternary complexes with 3-PG (10 mM) plus MgATP (10 mM) were measured using a MAR345 Image Plate at a sample-detector distance of 2.4 m and wavelength of 1.5 Å, covering the momentum transfer range $0.012 < s < 0.45$ Å^{-1} ($s = 4\pi\sin(\theta)/\lambda$, where 2θ is the scattering angle). The data were processed by PRIMUS [15] and the scattering patterns from the atomic models of the X-ray coordinates were computed using CRYSOL [16].

2.9. Molecular graphical analysis

For the analysis of PGK structures (pdb codes: **13PK** (*Trypanosoma brucei* PGK*3PG*MgADP [17]) and **1VPE** (*Thermotoga maritima* PGK*3PG*MgAMP-PNP [18])) the Insight II (Biosym/MSI, San Diego, CA) software was used. The limiting values for H-bond, hydrophobic and ionic interactions are considered to be 3.5, 4.5 and 4.0 Å, respectively.

3. Results and discussion

3.1. Effects of mutations on the catalytic efficiency of hPGK

The present mutations of hPGK had no any or only very slight effects on the binding (K_d) of each substrate (not shown), as tested by the method, previously elaborated by us [10], but the kinetic parameters are much more affected (Table 1). Among the single Ala mutants T393A exhibited the largest (about two orders of magnitude) loss in the catalytic efficiency (k_{cat}/K_m) compared to the wild-type enzyme. This indicates the importance of T393 in operation of the assumed hinge at βL. Furthermore, the single mutants of S392, F165, E192 and F196 possess variously diminished catalytic efficiencies, thus cumulative effects of these residues can be assumed. The double mutant S392A–T393A accumulates the properties of both single mutants of S392A and T393A, in accordance with the assumed cumulative effects. Only the catalytic efficiency of S398A is comparable to that of the wild-type hPGK.

The results with T393A mutant support the previous suggestion about the role of T393 in communication between the domains. It was observed in PGK X-ray structures, containing

Table 1
Summary of the functional and the stability properties of the wild-type and mutant hPGKs

Constants[a]	PGK forms								
	hPGK[b]	F165A	E192A	F196A	S392A	T393A	S398A	S392A–T393A	T393del
Kinetic									
Reverse direction									
k_{cat}	833 ± 50	270 ± 20	155 ± 3	610 ± 20	575 ± 2	58 ± 3	200 ± 2	16.4 ± 0.7	0.067 ± 0.050
K_m^{MgATP}	0.11 ± 0.02	0.83 ± 0.07	0.24 ± 0.01	0.33 ± 0.02	0.078 ± 0.041	0.86 ± 0.15	0.030 ± 0.003	0.66 ± 0.05	0.13 ± 0.04
K_m^{3PG}	0.05 ± 0.02	0.95 ± 0.08	0.53 ± 0.09	0.69 ± 0.05	0.32 ± 0.19	0.99 ± 0.06	0.062 ± 0.010	1.66 ± 0.13	0.11 ± 0.05
k_{cat}/K_m^{MgATP}	$7.6 * 10^6$	$3.3 * 10^5$	$6.5 * 10^5$	$1.8 * 10^6$	$7.4 * 10^6$	$6.7 * 10^4$	$6.7 * 10^6$	$2.5 * 10^4$	$5.2 * 10^2$
k_{cat}/K_m^{3PG}	$1.7 * 10^7$	$2.8 * 10^5$	$2.9 * 10^5$	$8.8 * 10^5$	$1.8 * 10^6$	$5.9 * 10^4$	$3.2 * 10^6$	$9.9 * 10^3$	$6.1 * 10^2$
Forward									
k_{cat}	2630 ± 420	1170 ± 330	1130 ± 50	n.d.	n.d.	250 ± 20	n.d.	n.d.	n.d.
K_m^{MgADP}	0.12 ± 0.02	0.12 ± 0.02	0.09 ± 0.03	n.d.	n.d.	0.10 ± 0.03	n.d.	n.d.	n.d.
$K_m^{1,3BPG}$	0.0005 ± 0.0002	0.017 ± 0.005	0.0091 ± 0.0020	n.d.	n.d.	0.010 ± 0.002	n.d.	n.d.	n.d.
DSC (T_m)[c]	327.9	322.2	323.1	324.5	324.8	327.3	326.3	325.1	326.6

[a] Rate and equilibrium constants are given in s^{-1} and mM, respectively and k_{cat}/K_m values are expressed as $M^{-1}\,s^{-1}$.
[b] Data from Ref. [10].
[c] T_m (K) values are determined from the type of experiments shown in Fig. 3A.

bound 3-PG, that the side-chain of R38, besides participating in 3-PG binding, creates a contact with T393, either with the backbone of T393 [3,17] (Fig. 2A) or with the side-chain itself [18] (Fig. 2C). This is a plausible way of communication between the two domains and of the transmission of the conformational effect of 3-PG from its binding N-domain to the hinge at βL, as illustrated by the blue arrows in Fig. 2A and C. The greatly decreased k_{cat} of T393A and its increased K_m-value for 3-PG clearly support the participation of T393 in this process. The route of communication is through R38, which transmits the effect of 3-PG to T393, located in βL. According to the X-ray pictures (Fig. 2A and C) S392 is also involved in the transmission of 3-PG effect, in agreement with the increased K_m-value of S392A for 3-PG.

In contrast, removing the side-chain of S398 does not significantly modify the catalytic efficiency, thus the assumed role of this side-chain in operation of the main hinge can be excluded. This result also reveals that the S392–S398 contact (observed only in the X-ray structures of the PGK containing bound ADP [5,17] (Fig. 2A and B)) is irrelevant in respect of functioning.

Besides T393, the side-chains of F165, E192 and F196 are involved in operation of the hinge, since their mutations led to substantial decrease of all the k_{cat}/K_m values (Table 1). The K_m values for 3-PG is better increased than those for MgATP, thus, these residues may better contribute to mediating the 3-PG caused conformational effect towards βL. Fig. 2B and D depicts the structural details of this transmission from the 3-PG binding site to the bending region. 3-PG is linked to α5 through the interaction of its 3-phosphate with R170 and the conserved F165 of α5 interacts with E192 of α7 of the interdomain region in all known PGK structures. Furthermore, E192 interacts permanently with the side-chains of S392 and H390, the constituting residues of βL. Thus, E192 and F165 are key residues in transmitting the effect of 3-PG towards the main hinge. Besides, E192 and F165 are also key residues in maintaining the structural integrity of the whole PGK molecule (cf. below).

We have also prepared a deletion mutant with lacking of the residue T393 that caused a dramatic activity loss. This underlines the importance not only the side-chain of T393 itself, but also the proper shape and length of the βL in the catalytic function, too. The deletion caused at least four orders of magnitude loss in the catalytic efficiency, but the interaction with the substrates has not been changed. Thus, βL has no direct role in substrate binding, but its intact main-chain is essential for the function. These findings, clearly support our previous hypotheses [6,7] about the role of βL in functioning of PGK.

3.2. *Effects of mutations on the structural integrity of hPGK: calorimetric and thiol-reactivity studies*

To detect any effect of mutations on the enzyme structure and stability, CD and DSC measurements were carried out. While CD spectra did not indicate any substantial change in the secondary structure of either mutants compared to the wild-type enzyme (not shown), the calorimetric melting curves detected destabilization effects upon mutations of F165A and E192A (Fig. 3A). In both cases the melting temperatures decreased by about 5 K and the transition curves exhibited less cooperativity. In agreement, loosening of the whole protein structure of F165A and E192A mutants was indicated by an increased reactivity of their buried thiol-groups (Fig. 3B). The hPGK possess two fast-reacting and five slow-reacting buried thiols [13]. The reaction of the slow-reacting thiols is limited by a first-order conformational change, which becomes remarkably faster for both mutants of F165A and E192A (Fig. 3B). Multiple interactions of F165 and E192 (Fig. 2C and D) make the above findings understandable. Substrates can counterbalance the loosening effects by mutations, as indicated by regaining the diminished reactivity of the

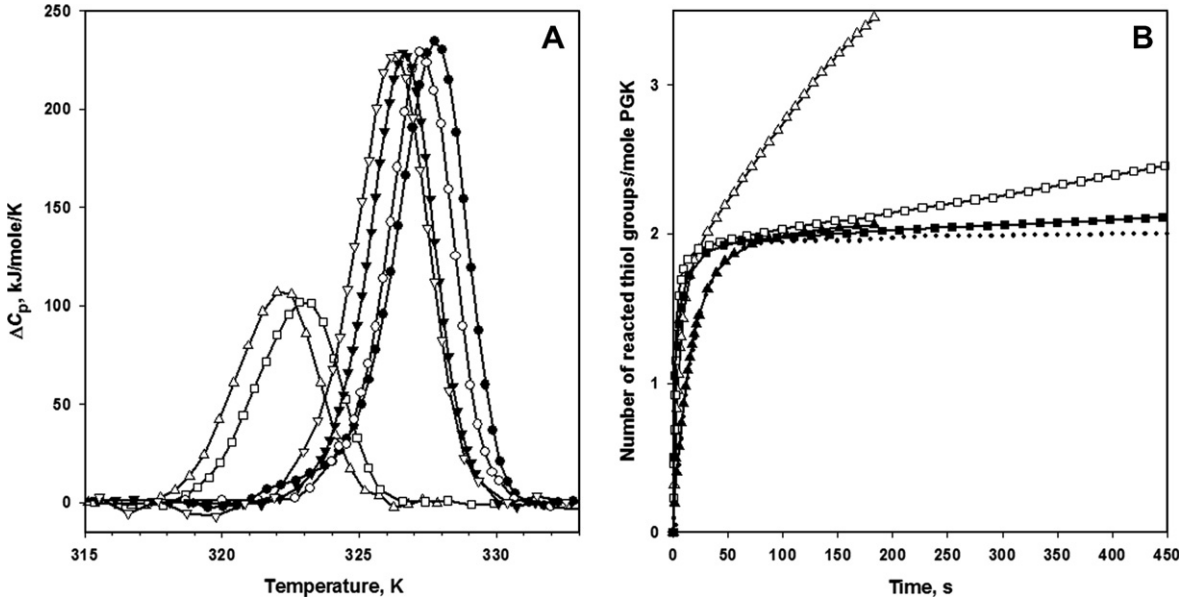

Fig. 3. Effect of mutations on thermal stability (A) and thiol reactivity of hPGK (B). DSC heat transition curves of the substrate-free wild-type (●), T393A (○), T393del (▼), S398A (▽), E192A (□) and F165A (△) mutant hPGKs are shown in panel A. In panel B, the reaction of 9 μM wild-type (dotted line), E192A (□) and F165A (△) mutant hPGKs with 0.05 mM Nbs_2 was followed. The mutants were also investigated in the presence of 10 mM 3-PG: E192A (■) and F165A (▲). The number of reacted thiol-groups per mole hPGK was calculated using ε_{412} of 14150 M^{-1} cm^{-1} [13] and plotted against the reaction time.

Table 2
Comparison of SAXS experimental parameters with those of the crystallographic models[a]

SAXS experiments			Discrepancy values between the scattering from crystallographic models and experimental data					
Investigated PGK forms	R_g (experimental) (Å)		Open crystal structures				Closed crystal structures	
	GNOM method	Guinier method	Pig PGK (no ligand)	Bs PGK MgADP binary	Pig PGK MgATP binary	Pig PGK 3-PG binary	Tm PGK ternary1[c]	Tb PGK ternary2[c]
Wild-type	22.5 ± 0.5	23.0 ± 0.2	6.14	6.04	4.66	5.31	2.25	**1.61**
E192A	23.7 ± 0.3	23.9 ± 0.2	2.89	3.01	**1.99**	2.27	2.79	3.43
S392A	23.8 ± 0.2	24.1 ± 0.3	1.45	1.78	1.68	**1.43**	2.44	2.40
T393A	23.7 ± 0.3	24.0 ± 0.2	2.77	3.72	2.35	**2.11**	2.93	2.94
S392A–T393A	23.9 ± 0.2	24.1 ± 0.2	2.71	3.99	2.51	**1.97**	3.55	3.76
T393del	23.8 ± 0.2	24.1 ± 0.3	**1.27**	1.45	1.29	1.28	1.83	1.95
S398A	22.7 ± 0.3	23.0 ± 0.2	3.99	4.02	3.25	3.45	1.96	**1.40**
R_g (theoretical) (Å)[b]			24.25	24.34	24.02	23.97	23.26	22.64
Molecular mass (kDa)[b]			43.7	43.2	43.6	43.8	43.7	45.3

[a]The minimum values of discrepancy (in bold) indicate the best correlation between SAXS data and crystallographic model.
[b]Radius of gyration (R_g) and molecular mass of the high resolution models as retrieved from the PDB. PDB codes: 1PHP for *Bacillus stearothermophilus* (Bs) PGK∗MgADP, 1VJC for *pig* PGK∗MgATP, 1VPE for *Thermotoga maritima* (Tm) PGK ternary and 13PK for *Trypanosoma brucei* (Tb) PGK ternary complexes. The PDB co-ordinates of *pig* substrate-free structure and PGK∗3-PG binary complex [3] were obtained from the authors.
[c]Ternary1 and ternary2 denote MgAMP-PNP∗3-PG and MgADP∗3-PG ternary complexes, respectively.

slow-reacting thiols upon substrate binding to these mutants (Fig. 3B) and by the fact that both mutants exhibit relatively good catalytic activities (Table 1).

3.3. Effects of mutations on the substrate-caused domain closure of hPGK: SAXS experiments

We have tested how the mutations influenced the substrate-caused conformational changes. The previous SAXS data with wild-type PGK demonstrated that both substrates together cause the largest change in the enzyme conformation, by inducing domain closure [7]. Here we carried out measurements with most of the hinge-region mutants and the results are summarised in Table 2. Only the S398A mutant undergoes complete domain closure upon binding of both substrates, similar to the wild-type hPGK. This finding correlates well with the native-like kinetic properties of S398A mutant (Table 1). For all other mutants (except T393del) an intermediate situation, partial domain closure can be deduced from the analysis of the SAXS scattering curves (Table 2) and this coincides with the partial catalytic activities of these mutants, indicating that neither of the corresponding side-chains is responsible alone for functioning of the molecular hinge at βL. The results with the mutant T393del clearly suggest the absence of the occurrence of domain closure, in agreement with its highly reduced catalytic activity.

3.4. General conclusions

It is not yet decided whether occurrence of domain closure obeys to the ligand driven model [19] or this conformational transition can occur even in the absence of substrates [2]. We have no experimental data for the occurrence of the conformational transition of PGK in the absence of substrates. Molecular dynamic simulations, however, indicates the occurrence of domain motion at the time scale of nanoseconds even for the substrate-free enzyme [20]. Our results with hPGK are entirely consistent with the assistance of substrates (especially, 3-PG) in contributing domain movement during the catalytic cycle.

A further conclusion is that the cumulative effects of multiple interactions of the side-chains in the hinge-region, rather than individual residues are likely to be responsible for the efficient mechanism of ligand-induced domain movement.

Acknowledgements: The financial support by the Grants OTKA (NI 61915 and D 048578) of the Hungarian National Research Fund, the Grant GVOP-3.2.1. 2004-04 0195/3.0, as well as the travelling grants for B.F., J.Sz. and A.V. were provided by the European Community – Research Infrastructure Action under the FP6 "Structuring the European Research Area Programme" contract number RII3/CT/2004/5060008, are gratefully acknowledged. D.S. and P.K. acknowledge support from the EU Design Study "SAXIER", contract no. 011934. The PDB data for the substrate-free PGK are acknowledged to Z. Kovári (ELTE University).

References

[1] Bahar, I., Chennubhotla, C. and Tobi, D. (2007) Intrinsic dynamics of enzymes in the unbound state and relation to allosteric regulation. Curr. Opin. Struct. Biol. 17, 633–640.
[2] Henzler-Wildman, K.A., Lei, M., Thai, V., Kerns, S.J., Karplus, M. and Kern, D. (2007) A hierarchy of timescales in protein dynamics is linked to enzyme catalysis. Nature 450, 913–916.
[3] Harlos, K., Vas, M. and Blake, C.C.F. (1992) Crystal structure of the binary complex of pig muscle phosphoglycerate kinase and its substrate 3-phospho-D-glycerate. Proteins 12, 133–144.
[4] Flachner, B., Kovári, Z., Varga, A., Gugolya, Z., Vonderviszt, F., Náray-Szabó, G. and Vas, M. (2004) Role of phosphate chain mobility of MgATP in completing the 3-phosphoglycerate kinase catalytic site: binding, kinetic, and crystallographic studies with ATP and MgATP. Biochemistry 43, 3436–3449.
[5] Davies, G.J., Gamblin, S.J., Littlechild, J.A., Dauter, Z., Wilson, K.S. and Watson, H.C. (1994) Structure of the ADP complex of the 3-phosphoglycerate kinase from *Bacillus stearothermophilus* at 1.65 A. Acta Crystallogr. D 50, 202–209.
[6] Szilágyi, A.N., Ghosh, M., Garman, E. and Vas, M. (2001) A 1.8 A resolution structure of pig muscle 3-phosphoglycerate kinase with bound MgADP and 3-phosphoglycerate in open conformation: new insight into the role of the nucleotide in domain closure. J. Mol. Biol. 306, 499–511.
[7] Varga, A., Flachner, B., Konarev, P., Gráczer, É., Szabó, J., Svergun, D., Závodszky, P. and Vas, M. (2006) Substrate-induced double sided H-bond network as a means of domain closure in 3-phosphoglycerate kinase. FEBS Lett. 580, 2698–2706.
[8] Mas, M.T., Bailey, J.M. and Resplandor, Z.E. (1988) Site-directed mutagenesis of histidine-388 in the hinge region of yeast

3-phosphoglycerate kinase: effects on catalytic activity and activation by sulfate. Biochemistry 27, 1168–1172.
[9] Joao, H.C., Taddei, N. and Williams, R.J. (1992) Investigating interdomain region mutants Phe194----Leu and Phe194----Trp of yeast phosphoglycerate kinase by 1H-NMR spectroscopy. Eur. J. Biochem. 205, 93–104.
[10] Flachner, B., Varga, A., Szabó, J., Barna, L., Hajdú, I., Gyimesi, G., Závodszky, P. and Vas, M. (2005) Substrate-assisted movement of the catalytic Lys 215 during domain closure: site-directed mutagenesis studies of human 3-phosphoglycerate kinase. Biochemistry 44, 16853–16865.
[11] Furfine, C.S. and Velick, S.F. (1965) The acyl–enzyme intermediate and the kinetic mechanism of the glyceraldehyde 3-phosphate dehydrogenase reaction. J. Biol. Chem. 240, 844–855.
[12] Szilágyi, A.N. and Vas, M. (1998) Anion activation of 3-phosphoglycerate kinase requires domain closure. Biochemistry 37, 8551–8563.
[13] Cserpán, I. and Vas, M. (1983) Effects of substrates on the heat stability and on the reactivities of thiol groups of 3-phosphoglycerate kinase. Eur. J. Biochem. 131, 157–162.
[14] Roessle, M.W. et al. (2007) Upgrade of the small-angle X-ray scattering beamline X33 at the European Molecular Biology Laboratory, Hamburg. J. Appl. Crystallogr. 40, s190–s194.
[15] Konarev, P.V., Volkov, V.V., Petoukhov, M.V. and Svergun, D.I. (2006) ATSAS 2.1, a program package for small-angle scattering data analysis. J. Appl. Crystallogr. 39, 277–286.
[16] Svergun, D.I., Barberato, C. and Koch, M.H.J. (1995) CRYSOL – a program to evaluate X-ray solution scattering of biological macromolecules from atomic coordinates. J. Appl. Crystallogr. 28, 768–773.
[17] Bernstein, B.E. and Hol, W.G. (1998) Crystal structures of substrates and products bound to the phosphoglycerate kinase active site reveal the catalytic mechanism. Biochemistry 37, 4429–4436.
[18] Auerbach, G., Huber, R., Grättinger, M., Zaiss, K., Schurig, H., Jaenicke, R. and Jacob, U. (1997) Closed structure of phosphoglycerate kinase from *Thermotoga maritima* reveals the catalytic mechanism and determinants of thermal stability. Structure 5, 1475–1483.
[19] Hayward, S. (2004) Identification of specific interactions that drive ligand-induced closure in five enzymes with classic domain movements. J. Mol. Biol. 339, 1001–1021.
[20] Balog, E., Laberge, M. and Fidy, J. (2007) The influence of interdomain interactions on the intradomain motions in yeast phosphoglycerate kinase: a molecular dynamics study. Biophys. J. 92, 1709–1716.